Journal of Thermal Analysis and Calorimetry, Vol. 86 (2006) 1, 243–248

MODELLING OF A HIGH PRESSURE CALORIMETER
Application to the measurement of the latent heat of a model food (tylose)

A. Ousegui[1], *S. Zhu*[2], *H. S. Ramaswamy*[2] *and A. Le Bail*[1]*

[1]UMR GEPEA (UA CNRS 6144-SPI), ENITIAA, Rue de la Géraudière BP 82225, 44322 Nantes Cedex 03, France
[2]Department of Food Science and Agricultural Chemistry, McGill University, 21111 Lakeshore Road, Ste Anne de Bellevue Quebec H9X 3V9, Canada

The evaluation of the latent heat and enthalpy of fusion of food systems in the case of high pressure–low temperature processing is important for modelling purposes as well as for technical applications. A high pressure calorimeter has been designed for this purpose. The high pressure calorimeter was used to evaluate the latent heat during a pressure scan at constant temperature. It permits to measure the heat of phase transitions and to obtain the relationship between the initial freezing temperature T_{ifp} and the average pressure while the phase transition is going on.

This work presents a modelling of results obtained from an experimental approach using a high pressure calorimeter and from a mathematical model developed from existing data on the phase change of pure water.

The modelling work consisted in evaluating the latent heat measured in previous tests from computations taking into account the dependence of the latent heat of fusion of water on pressure. Models predicting the amount of frozen water in a food matrix under atmospheric conditions were used to determine the initial amount of frozen water in the sample. Then a stepwise procedure was operated in a program to reproduce the pressure rise occurring during a high pressure calorimeter test. The amount of melted ice at each pressure step was calculated using conventional ice fraction models, which were adapted to pressure dependence of the initial freezing temperature and the dependence of the latent heat pressure. The comparison was satisfactory, especially at low temperatures.

Keywords: *calorimetry, high pressure, initial freezing temperature, latent heat, phase transition*

Introduction

High pressure (HP) processes at sub zero temperatures is attracting research efforts. Its implementation in the food industry seems to be of interest to manage high pressure assisted freezing or thawing processes. The depression of the initial freezing temperature with pressure suggests the possibility of new applications in the area of food process [1], such as pressure assisted freezing, pressure assisted thawing (PAT), pressure shift freezing (PSF), pressure induced thawing (PIT), etc.

PAF (ABCD in Fig. 1) has been applied to food systems, and results in reduced drip losses accompanied by an improved texture with respect to unfrozen samples. This has been demonstrated by several researchers in the case of tofu [2, 3], for fruits and vegetables [4] and for bovine muscle [5].

PAT (DCBA in Fig. 1) might also result in a reduction of the drip losses with respect to atmospheric thawing although this result was not obvious. A study on PAT of tuna by (Deuchi and Hayashi 1992) showed that a reduction of the drip was possible. The same technique implicated to ground beef resulted in a significant change in meat colour with less thawing time [6].

HP process might either enhance or reduce enzymatic activity [7] defined the *T–P* diagram of protein denaturation [1, 8, 9].

PSF (AEFG in Fig. 1) was the subject of many studies. Most of them focus on the advantageous effects on texture and structure of products. PSF resulted in a better structure than their air blast frozen counterparts [2]. Damage is compared to the microstructure of eggplants frozen by conventional air freezing and by PSF [10]. PSF processed samples had fresh appearance and no differences between center and surface cell structure were observed (indicating the uniform nucleation). The same remarks were evocated [11] for large meat pieces of pork muscle. PIT (GFEA in Fig. 1) is another technique in HP area. Many studies concluded that the most important advantages of this technique is the reduction of treatment time [12–14].

More details to HP process and his potential applications exist in the literature [15–17].

Understanding pressure–dependent phase change phenomena is quite important for a better development of these new technologies [18]. Foods mainly contain water, almost all existing knowledge is related to pure water, whereas very few data concern real food systems. The International Association for the Properties

* Author for correspondence: lebail@enitiaa-nantes.fr

1388–6150/$20.00

Akadémiai Kiadó, Budapest, Hungary
Springer, Dordrecht, The Netherlands

of Water and Steam (IAPWS) adopted a new general and scientific use [19], valid in stable fluid region of water from the melting–pressure curve to 1000°C, at pressure up to 1000 MPa. The freezing domain is not concerned by this database. Semi-empirical expressions are proposed [20] for specific volume, specific isobaric heat capacity, isothermal compressibility coefficient, and thermal expansion coefficient of water and ice [21–23] determined experimentally the thermal conductivity, thermal coefficient and density of canned tomato paste and apple pulp up to 400 MPa, also the latent heat of fusion of tylose [22]. Phase diagram and the melting latent heat of fusion of KCl aqueous solutions are determined [24] with a constant mass isothermal HP calorimeter.

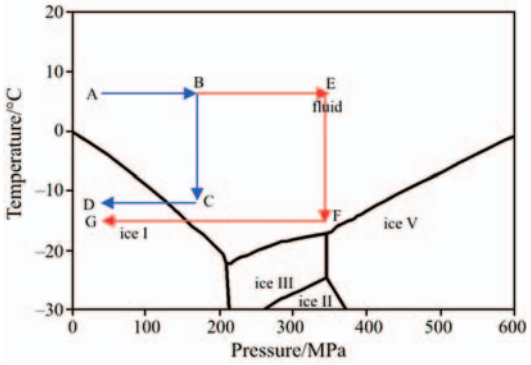

Fig. 1 Possibilities and definitions of high pressure processing on phase transition of water

More recently, a high pressure calorimetry was developed to measure the latent heat of fusion of selected food substances during a pressure scan at constant temperature [25, 26]. The phase change in the calorimeter is monitored by a pressure scan at constant temperature. In the case of food, ice crystallisation is spanned over a given temperature interval. This calorimeter has been presented in previous study [27].

Data were recently obtained with tylose as a model system and we give them for the first time in this paper.

The objective of this paper is to develop a mathematical model that reproduces the temperature and pressure excursion of a given sample in this calorimeter. This model could thereafter be used to explain and support the theory of phase transition occurring in this high pressure calorimeter.

Experimental

Methods and materials

High pressure calorimetric system

A HP differential scanning calorimeter (DSC) (Fig. 2) was used in this study. The experimental system consisted in a differential calorimetry head, a refrigerated circulator, two HP cells, a HP compressor and a computer. The calorimetry head (Pass 27, Sceres, Orsay, France) had two cavities (20 mm diameter×95 mm depth) used for holding the sample and the reference cells. There were 220 thermocouple junctions installed between the two cavities to amplify the generated temperature differential signal. Two platinum temperature sensors (Pt 100) were placed under each of the cavities to monitor/control the temperature of the calorimeter. The temperature of the calorimetry head was controlled through a copper coil winding around the contour of the head (Fig. 2a) and an oven around the system. The copper coil was connected to the refrigerated circulator (Huber CC250, Offenburg, Germany) with a water–glycol medium. During the experiment, the calorimetric head together with the copper coil was thermally insulated in a plastic box containing foamed plastics.

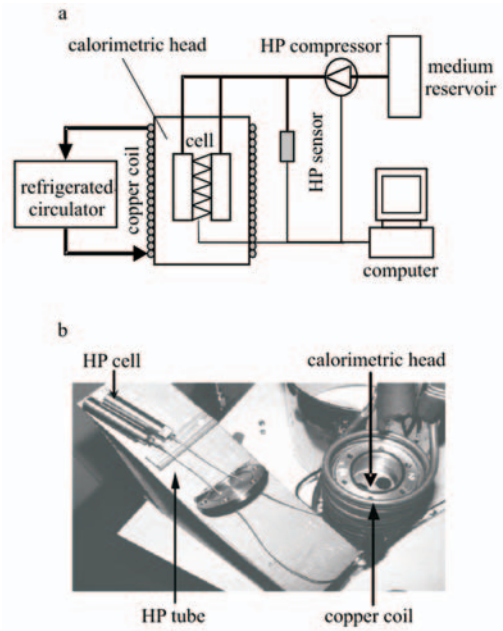

Fig. 2 Experimental set-up of HP calorimeter: a – schematic diagram and b – photograph of the calorimetric head and the cells

The HP cell (made of beryllium copper) contained two plugs with nitrile O-ring and a threaded bolt for sealing on one side (Fig. 3). It was connected to a pressure tube (3.2 mm diameter) on the other side with miniature fittings (M2 Serie, 100 MPa, Harwood Engineering, MA).

The pressure within the system was achieved through the HP compressor (400 MPa, 5 cm^3, Nova-Swiss, Effretikon, CH) driven by a step motor (MO63-LE09, Mijno, Fenwick, France) and controlled by the computer. A pressure sensor (200 or 400 MPa, Asco Instruments, Chateaufort, France)

was used to monitor and control the pressure. When the pressure required for a test exceeded 180 MPa, the 400-MPa sensor was used during the experiment. A software (Labview 6, National instruments, Austin, TX) was used for system control and data recording (temperature, pressure and heat flow). Pentane (Sigma, Fallavier, France) was used as pressurization medium in the system because of its stability over the whole tested pressure range and its properties (low viscosity, no phase transition) [28]. Full details of this equipment and of its validation in the case of pure water are proposed [25, 26].

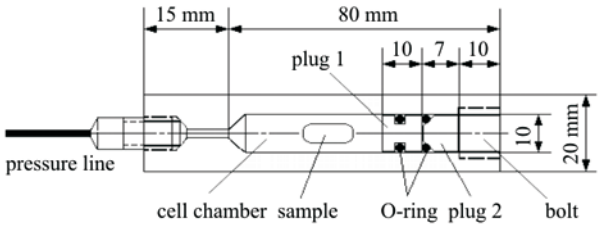

Fig. 3 High-pressure cell and sample installation

Calibration

The pressure sensor was calibrated *vs*. a reference pressure gauge (Bourdon, France). The temperature of the calorimeter was calibrated against a K-type thermocouple (0.1 mm diameter, Omega, USA) placed in the sample cell at selected temperature between –20 and 20ºC. The calorimeter was calibrated using a 100 Ω resistance located in the sample cell. A voltage in the range from 1.0 to 4.2 V was supplied to this resistance by a power source (220 programmable voltage source, Keithley Instruments SARL, Saint-Aubin, France) for period between 30 and 90 min. The heat generated by the resistance was calibrated on hand of the measured voltage and current respectively with a voltmeter (7055 Voltmeter, Solartron Mobrey SA, Saint-Christophe, France) and an ampere meter (195A multimeter, Keithley Instruments, SARL, Saint-Aubin, France). The calorimetric differential temperature signal (mV) due to the electric heating was recorded every 5 s. The peak area was then integrated to calculate the ratio of heat power to calorimetric voltage at selected temperatures. The calibration tests were carried out from –20 to 20°C. A linear fit of the experimental data was obtained as:

$$q=ks=(37.09+0.0772T)s \quad (R^2=0.978,\ n=8) \quad (1)$$

where q is heat flow rate (mW), s is calorimetric signal (mV), k is the ratio of heat flow rate to calorimetric signal (mW mV^{-1}), T is the temperature of the calibration tests performed (°C). Similar calibration procedures have been used in [27, 29].

Sample preparation

Tylose was purchased from (MADI S.n.c., Tavazzano con Villavesco (LO), Italy. Small samples of Tylose were prepared for HP calorimetric experiments. Each specimen was vacuum-packaged in a polyethylene bag (80 μm thick multiplayer film) (La Bovida, Nice, France). Packaged samples were stored in a cooler (4°C) before the experiments. For the test, the sample was installed in the sample cell (Figs 2a and b). The reference cell was prepared in the same way as the sample cell but without the sample. Air bubbles were carefully removed from the cell during the preparation of both sample and reference cells. After calorimetric experiments, the moisture content (77.9±0.3%, mean±standard deviation) was determined for each test sample using a drying oven at 103°C for 24 h.

Isothermal pressure-scan (*P*-scan)

After sample installation, the sample and reference cells were placed in the sample and reference cavities, respectively. The sample was frozen at the set temperature (–5, –6.9, –10, –15, –18ºC) in the calorimeter. Once the calorimeter signal showed a stable baseline (close to zero), the pressure was increased from the atmospheric level (0.1 MPa) at a constant rate (0.3 MPa min^{-1}) and the heat flow signal was recorded every 5 s. Once the pressure is high enough to start melting at the studied working temperature, the frozen sample starts melting, resulting in an endothermic peak as shown in Fig. 4. The pressure scan rate used in this study was relatively low as compared with that in Le Bail *et al*. (2001). This was just for obtaining a better heat flow signal (sharper and deeper downward peak, less delay).

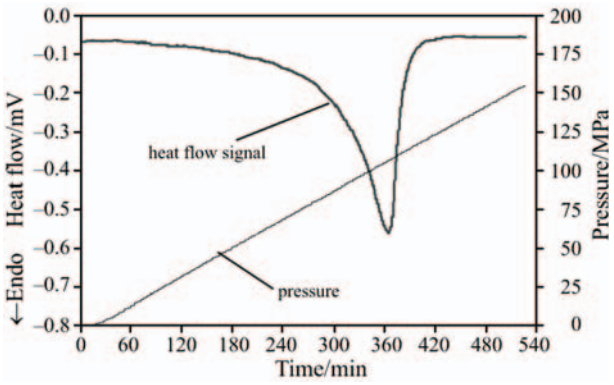

Fig. 4 A typical measurement of isothermal pressure scan (0.3 MPa min^{-1}) of tylose (0.5157 g) with calorimetric temperature at –10°C

Heat transfer model during a calorimeter run

Thermal properties I

The tylose is presented as a two-phase material, which consisted in a solid phase (ice crystals) and a continuous phase made of dry matter and unfrozen water. While noting X_{wt} the total percentage of water in the tylose and T_{ifp} the initial freezing, the amount of ice formed at a temperature $T<T_{ifp}$ is given by equation [30]:

$$X_{ice}=(X_{wt}-X_{unf})\left(1-\frac{T_{ifp}}{T}\right)\Big/\left(1-\frac{T_{ifp}}{T_{ref}}\right) \quad (T \text{ in } °C) \quad (2)$$

where T_{ref} represents the temperature below which the totality of water being able to be frozen, is in the ice form. Equation (2) is valid at P_{atm}, and was extrapolated under high pressure to estimate X_{ice}. the values obtained at atmospheric pressure will be shifted at HP according to the evolution of T_{ifp} *vs*. pressure. Figure 5 shows the application of this equation to the case of tylose.

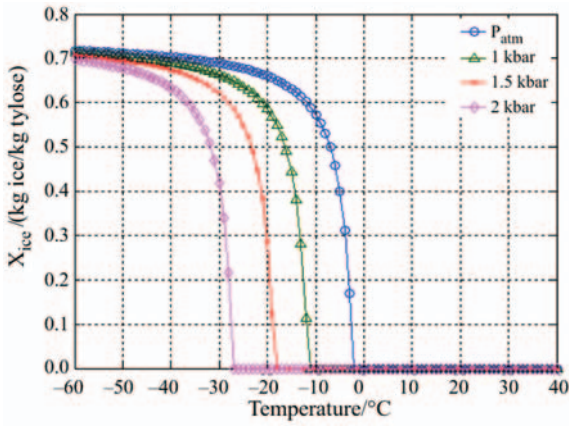

Fig. 5 Evolution of ice content in tylose for different pressures using shift approach

Modelling of a pressure scan and prediction of the latent heat of fusion

A high pressure calorimetry run usually starts after equilibration of the temperature of the sample at a given temperature and at atmospheric pressure. According to the curve of the ratio of frozen water at atmospheric pressure (Figs 5 and 6), it is obvious that the sample was in fact partially melted. Therefore, the amount of energy that will be measured by the calorimeter to ensure the melting of the sample during an isothermal compression will represent a part of the energy needed to thaw the ice present in a sample that would be fully frozen. Initially the tylose is at the temperature T_0 and atmospheric pressure P_0. The application of Eq. (2) permits to evaluate the initial amount of water that is frozen (X_0). Isothermal compression causes a reduction of the amount of frozen water (i.e. X_1 at P_1 and T_0) as shown in Fig. 7.

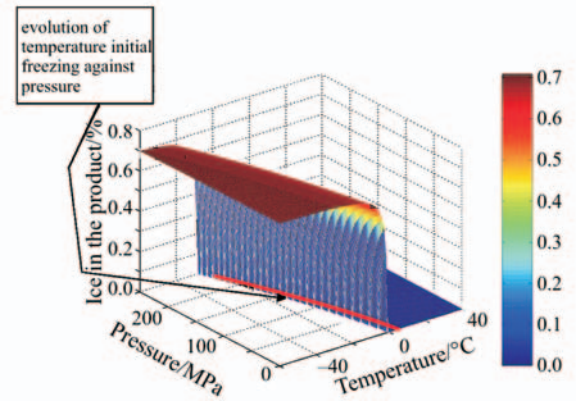

Fig. 6 Ice content evolution *vs*. pressure and temperature

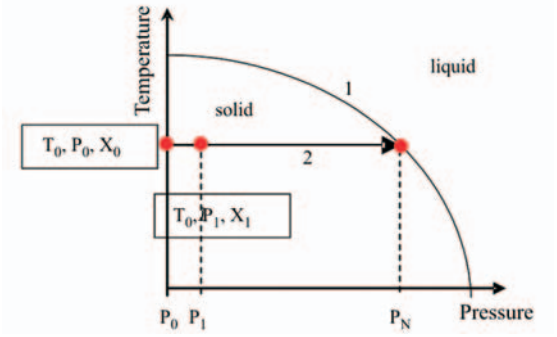

Fig. 7 Pathway of the isothermal compression: 1 – the frontier of the end of melting, 2 – compression process

$(X_0–X_1)$ represents the amount of melted water during a pressure step $P_0–P_1$. This melting requires the following energy:

$$L_m=(X_1–X_0)L(P_1) \quad (3)$$

where $L(P_i)$ is the water latent heat of fusion of pure water at the pressure P_i and is given by [28]:

$$L \text{ (J g}^{-1})=333–0.399P+0.000388P^2 \ (P \text{ in MPa}) \quad (4)$$

The model was using Eqs (3) and (4) to determine the amount of energy taken by the sample during a pressure step between pressure P_0 and pressure P_1. The computation was realised using steps of 1 MPa until the full melting of the sample P_N. Thermodynamic equilibrium was supposed to be obtained between each pressure step.

Results and discussion

Figure 4 shows a typical example of endothermic heat flow signal recorded during the *P*-scan test of tylose, at a calorimetric temperature of –10°C. As the pressure increased, the endothermic (heat flow), calorimetric peak started develop more, because of continued melting of ice in tylose. The latent heat per gram of tylose (L_m) was evaluated using calorimetric signal peak and average pressure ($\overline{P}_{1-2}$) [16, 29].

Table 1 Calculated *vs*. experimental tylose enthalpy for selected temperatures and average pressures

T/ °C	$\overline{P}_{1-2}$/ MPa	L_{m-cal}/ J g^{-1} tylose	L_{m-exp}/ J g^{-1} tylose	Error/%
–4.95	53.3	181.90	156	16.60
–5.00	78.6	182.24	155	17.57
–6.90	74.2	189.82	163	16.46
–6.90	73.7	189.82	158	20.14
–9.90	107.5	191.25	168	13.84
–10.15	107.1	191.08	175	9.19
–15.00	153.2	184.08	174	5.79
–15.10	153.0	183.89	178	3.31
–18.00	174.6	177.85	174	2.21
–18.00	175.2	177.85	177	0.48

The relationship between phase (Eq. (5)) transition temperature T_{ifp} and average pressure ($\overline{P}_{1-2}$) was deducted from the equation of pure water given by [28]:

$$T_{ifp}\ (°C)=(T_{tfp})_{atm}-0.072192\overline{P}_{1-2}-0.000155\overline{P}_{1-2}^{2} \quad (5)$$

The value of $T(T_{ifp})_{atm}$ has been determined experimentally and is equal to –1°C. Tables 1 and 2 present the comparison between the values obtained during the experiments and calculated by the model respectively for latent heat and ice mass fraction in the case of tylose. The relative error remains acceptable for the low temperatures (ca. below –10°C). The curve shape of ice formation (Fig. 5) shows that an error of 1°C of estimate or measurement of the temperature can lead to an error of 10% on calculation of the percentage of ice, which explains the great difference between the values experimental and simulated values obtained above ca. –10°C. The amount of melted water during the calorimeter test is presented in Table 2. It can be raised on the level of the percentage of the ice melted at the time of isothermal compression. The experimental percentage of ice that was thawed during the isothermal compression can be calculated using the relation:

$$(X_{ice})_{exp}=\frac{L_m\ (\mathrm{J\,g^{-1}\ tylose})}{L(\overline{P}_{1-2})\ (\mathrm{J\,g^{-1}\ water})} \quad (6)$$

This relation takes into account the latent heat of pure water at the mean pressure of the peak and therefore represents a mean value of the latent heat of water over the phase change peak. Beside, the calculated value indicated in Table 2 represents the amount of melted ice obtained during the pressure scan by calculation. A relatively good agreement was observed for these values.

Nevertheless, a larger discrepancy was observed once again for temperature above ca. –10°C confirming the results obtained in Table 1. These results exhibits the limits of high pressure calorimetry applied to phase change of water in biological systems (when temperature is above –10°C). This discrepancy can be explained by inaccuracy in the measurement of the sample temperature, in the pressure measurement and in the calibration. Indeed, the calorimeter head was calibrated in conditions that were not strictly isothermal due to the heat dissipated by the resistance.

Table 2 Calculated *vs*. experimental tylose ice percentage for selected temperatures and average pressures

T/°C	$\overline{P}_{1-2}$/MPa	X_{ice}^{cal}/%	X_{ice}^{exp}/%	Error/%
–4.95	53.3	57.34	50	13.63
–5.00	78.6	57.48	51	13.52
–6.90	74.2	61.48	56	9.98
–6.90	73.7	61.48	56	9.98
–9.90	107.5	64.66	61	5.90
–10.15	107.1	64.84	61	6.54
–15.00	153.2	67.15	65	2.99
–15.10	153.0	67.18	65	2.95
–18.00	174.6	67.96	66	2.21
–18.00	175.2	67.96	66	2.21

Conclusions

The evaluation of the energy required for the melting of a sample at a given initial temperature has been measured previously during a pressure scan using a high pressure calorimeter operated at constant temperature. The sample was partially frozen at the beginning of the pressure scan at constant pressure and the amount of melted water was taken into account. In our conditions, we observed that for the case of tylose, the amount of frozen water was between ca. 50 and 66% at –4.95 and –18°C, respectively. Therefore the amount of water that was melted and detected by the calorimeter during a pressure scan was only partial. A mathematical model was developed to calculate this expected latent heat measured by the calorimeter and was in a relatively good agreement with the measured values, especially for the low temperatures domain.

Nomenclature

L	latent heat of fusion of pure water (J g^{-1})
L_m	latent heat of fusion of tylose (J g^{-1})
P	pressure (MPa)
q	heat flow rate (mW)
s	instantaneous calorimetric signal (mV)
T	temperature (°C)
X	mass fraction

Subscripts

ifp	initial freezing point
ref	reference
unf	unfrozen water
wt	total water

Acknowledgements

This study was partially funded by the European Project of Safe Ice (QLK1-CT-2002-02230) and the Strategic Grants Program of the Natural Sciences and Engineering Research Council of Canada. The authors wish to thank L. Guihard and J. Laurenceau for their technical support during experimental work.

References

1 M. T. Kalichevsky, D. Knorr and P. J. Lillford, Trends Food Sci. Technol., 6 (1995) 253.
2 Y. Kanda, M. Aoki and T. Kosugi, J. Jpn. Soc. Food Sci. Technol. (pon Shokuhin Kogyo Gakkaishi), 39 (1992) 608.
3 M. Fuchigami and A. Teramoto, J. Food Sci., 62 (1997) 828.
4 N. U. Haase and B. Putz, Luft Kaelte Technik, 32 (1996) 310.
5 P. D. Sanz, C. D. Elvira, M. Martino, N. Zaritzky, L. Otero and J. A. Carrasco, Meat Sci., 52 (1999) 275.
6 Y. Zhao, R. A. Flores and D. G. Olson, J. Food Sci., 63 (1998) 272.
7 S. A. Hawley, Biochem., 10 (1971) 2436.
8 R. T. Hayashi, T. Kinsho and H. Ueno, High Pressure Food Science, Bioscience and Chemistry, Issac, Ed., The Royal Society of Chemistry, Cambridge UK 1998, pp. 166–174.
9 M. Hendrickx, L. Ludikhuyze, I. V. D. Broeck and C. Weemaes, Trends Food Sci. Technol., 5 (1998) 197.
10 L. Otero, M. T. Solas, P. D. Sanz, C. D. Elvira and J. A. Carrasco, Z. Lebensmittel Untersuchung Forschung A, 206 (1998) 338.
11 M. N. Martino, L. Otero, P. D. Sanz and N. E. Zaritzky, Meat Sci., 50 (1998) 303.
12 T. Deuchi and R. Hayashi, in High Pressure and Biotechnology, Colloque INSERM, C. Balny, R. Hayashi, K. Heremans and P. Masson, Eds, John Libbey Eurotext Ltd., London 1992, pp. 353–355.
13 A. LeBail, J. M. Chourot, P. Barillot and J. M. Lebas, Revue Générale du Froid, 1997 (972, avril 97), pp. 51–56.
14 D. Knorr, O. Schlüter and V. Heinz, Food Technol., 52 (1998) 42.
15 J. C. Cheftel, J. Levy and E. Dumay, Food Rev. Int., 16 (2000) 453.
16 A. LeBail, D. Chevalier, D. Mussa and M. Ghoul, Int. J. Refrigeration, 25 (2002) 504.
17 B. Li and D.-W. Sun, J. Food Eng., 54 (2002) 175.
18 L. Otero and P. D. Sanz, Innovative Food Sci. Emerging Technol., 4 (2003) 121.
19 IAPWS, International Association for the Properties of Water and Stream Relase on the IAPWS Formuulation 1995 for the thermodynamic properties of ordinary water substance for general and scientific use, Fredericia (Denmark), Copies of this and other IAPWS releases can be obtained from the Executive Secretary of IAPWS, Dr R. B. Dooley, Electric Power Research Institute, 3412 Hillview Avenue, Palo Alto, CA 94304, 1996.
20 V. E. Chizhov and O. V. Nagornov, Proceedings of the International Symposium, St. Petersburg 1991, September 1990, pp. 463–470.
21 S. Denys and M. E. Hendrickx, J. Food Sci., 64 (1999) 709.
22 S. Denys, A. M. V. Loey and M. E. Hendrickx, Biotechnol. Progr., 16 (2000) 447.
23 S. Denys, L. R. Ludikhuyze, A. M. V. Loey and M. E. Hendrickx, Biotechnol. Progr., 16 (2000) 92.
24 J. M. Chourot, A. LeBail and D. Chevalier, XXXVII Meeting of the European High Pressure Research Group, Montpellier, France, 9–11 September 1999.
25 S. Zhu, S. Bulut, A. Le-Bail and H. Ramaswamy, J. Food Proc. Eng., 27 (2004) 359.
26 S. Zhu, H. Ramaswamy and A. LeBail, J. Food Proc. Eng., 27 (2004) 377.
27 A. LeBail, D. Chevalier, J. M. Chourot and J. Y. Monteau, J. Therm. Anal. Cal., 66 (2001) 243.
28 P. W. Bridgman, Proceedings of the American Academy of Arts and Sciences, 47 (1912) 411.
29 J. M. Chourot, A. LeBail and D. Chevalier, High Pressure Res., 19 (2000) 191.
30 C. A. Miles, Meat freezing – Why and how?, MRI Symposium n°3, Langford 1974, Bristol, UK, April 1974: Meat Research Institute, Langford, Bristol UK, 16.1–16.10.

Received: August 20, 2005
Accepted: January 24, 2006

DOI: 10.1007/s10973-005-6963-6